HHS Public Access

Author manuscript

Proteomics Clin Appl. Author manuscript; available in PMC 2024 November 18.

Published in final edited form as:

Proteomics Clin Appl. 2024 September ; 18(5): e2300128. doi:10.1002/prca.202300128.

A novel micropeptide, *Slitharin*, exerts cardioprotective effects in myocardial infarction

Ahmed G. E. Ibrahim[1], **Alessandra Ciullo**[1], **Shukuro Yamaguchi**[1], **Chang Li**[1], **Travis Antes**[1], **Xaviar Jones**[1], **Liang Li**[1], **Ramachandran Murali**[2], **Innokentiy Maslennikov**[3], **Niveda Sundararaman**[1], **Daniel Soetkamp**[1], **Eugenio Cingolani**[1], **Jennifer Van Eyk**[1], **Eduardo Marbán**[1]

[1]Smidt Heart Institute, Cedars-Sinai Medical Center, Los Angeles, California, USA

[2]Department of Biomedical Sciences, Cedars-Sinai Medical Center, Los Angeles, California, USA

[3]Chapman University, School of Pharmacy, Irvine, California, USA

Abstract

Purpose: Micropeptides are an emerging class of proteins that play critical roles in cell signaling. Here, we describe the discovery of a novel micropeptide, dubbed slitharin (Slt), in conditioned media from Cardiosphere-derived cells (CDCs), a therapeutic cardiac stromal cell type.

Experimental design: We performed mass spectrometry of peptide-enriched fractions from the conditioned media of CDCs and a therapeutically inert cell type (human dermal fibrobasts). We then evaluated the therapeutic capacity of the candidate peptide using an in vitro model of cardiomyocyte injury and a rat model of myocardial infarction.

Results: We identified a novel 24-amino acid micropeptide (dubbed Slitharin [Slt]) with a non-canonical leucine start codon, arising from long intergenic non-coding (LINC) RNA 2099. Neonatal rat ventricular myocytes (NRVMs) exposed to Slt were protected from hypoxic injury in vitro compared to a vehicle or scrambled control. Transcriptomic analysis of cardiomyocytes exposed to Slt reveals cytoprotective capacity, putatively through regulation of stress-induced MAPK-ERK. Slt also exerted cardioprotective effects in rats with myocardial infarction as shown by reduced infarct size 48 h post-injury.

Correspondence: Ahmed G.E. Ibrahim, PhD, Smidt Heart Institute, Cedars-Sinai Medical Center, 8700 Beverly Blvd, 1090 Davis Bldg., Los Angeles, CA 90048, USA., Ahmed.Ibrahim@cshs.org.

AUTHOR CONTRIBUTIONS

Ahmed Gamal Ibrahim, Eugenio Cingolani, Travis Antes, Jennifer Van Eyk, and Eduardo Marbán conceptualization and supervision; Ramachandran Murali and Innokentiy Maslennikov analyzed data; Alessandra Ciullo, Chang Li, Xaviar Jones, Daniel Soetkamp investigation and data curation; Daniel Soetkamp, Travis Antes and Niveda Sundararaman proteomics; Ahmed Gamal Ibrahim and Eduardo Marbán writing-original draft.

CONFLICT OF INTEREST STATEMENT

EM owns founder's stock in Capricor Therapeutics. AI owns stock in Capricor Therapeutics. All other authors declare no conflicts of interest.

SUPPORTING INFORMATION

Additional supporting information can be found online in the Supporting Information section at the end of this article.

Conclusions and clinical relavance: Thus, Slt is a non-coding RNA-derived micropeptide, identified in the extracellular space, with a potential cardioprotective function.

Keywords

cardiomyocytes; cardiosphere-derived cells; micropeptide; myocardial infarction

1 | INTRODUCTION

Micropeptides are short (<100 amino acids) polypeptides that represent an emerging class of eukaryotic regulators [1, 2]. Micropeptides are classified according to their genomic origin. The first and best-described micropeptides, such as hormones and neurotransmitters, are cleavage products of larger proteins and transcripts. More recently, micropeptides have been found to arise from small open reading frames (sORFs) strewn across non-coding regions of the genome including 5′ untranslated regions (UTRs), long intergenic non-coding (LINC) RNAs, and polycistronic mRNAs of mitochondrial origin [3]. Functionally, micropeptides localize to various cellular compartments including the cytosol, nucleus, and plasma membrane, and bind a variety of substrates to regulate a diversity of processes including cell proliferation, calcium handling, and metabolic pathways [2, 4, 5]. Cardiosphere-derived cells (CDCs) are a population of cardiac stromal cells with demonstrated disease-modifying bioactivity in several models of tissue injury [6]. CDCs exert their therapeutic effects through paracrine means including the secretion of extracellular vesicles (EVs) and soluble factors to affect tissue repair [7]. Micropeptides remain poorly described in the context of EV signaling. To probe for micropeptides in the CDC secretome, we isolated small peptides from the conditioned media of this therapeutic cell type. Here, we describe the discovery of a novel micropeptide, dubbed slitharin (Slt), and its bioactivity.

Micropeptides from the conditioned media of human CDCs and a therapeutically inert control (human dermal fibroblasts) were enriched using polyethylene glycol (PEG) precipitation. EVs were lysed using surfactant and larger molecular weight proteins were filtered out using a 10 kDa molecular weight cutoff filter (with the flow-through retained). The remaining small peptides in the flow-flow through were digested with trypsin before tandem mass spectrometry (MS) (Figure 1A). Among the micropeptides uniquely expressed in CDC EVs from the potent donor were tryptic peptides that overlapped a 24 amino acid residue-long peptide which we dubbed *Slitharin* (Slt; Figure S1A–C). To determine whether Slt is a bona fide micropeptide (rather than a degradation or cleavage bi-product), we derived the RNA transcript from the amino acid sequence and conducted a Basic Local Alignment Search Tool (BLAST) to probe for its presence in the human transcriptome (Figure 1B). The RNA sequence for Slt mapped to the terminal end of LINC RNA 2099 (Figure 1B). Interestingly, the sequence for Slt begins with the triplet codon “cug” (leucine) instead of the canonical “aug” (methionine). However, translation initiation at non-methionine codons (including leucine) has been reported extensively [8–10]. Furthermore, the sequence for Slt is immediately flanked by termination (Stop) codon sequences confirming the full length of the peptide product (Figure 1B). Indeed, the Slt sequence was also detected (with some variation) in mammalian and avian species including primates and rodents (Figure S2A). Gene expression analysis showed enriched expression of Slt in three unique CDC donors

compared to normal skin fibroblasts (Figure 1C, Figure S2B). Slt presence was assayed in mouse brain, heart, kidney, liver, lung, and spleen tissue (Figure 1D, Figure S2C). Northern blot analysis identified two bands 0.5 kb and 80 bases in length which may reflect the full-length transcript and the mature transcript (Figure 1E). The presence of these transcripts was confirmed in human CDCs and several mouse tissues, and neonatal rat ventricular myocytes (NRVMs) suggesting the presence of the peptide transcript in three species. Presence of the 24-amino acid peptide was further confirmed using targeted MS detection of Slt in extracts from mouse heart, liver, and brain tissue (Figure 1F).

To evaluate the structure of Slt, we used nuclear magnetic resonance spectroscopy (NMR) of ^{13}C chemical shifts for Ca, Cb, and C° atoms in chemically synthesized Slt. These chemical shifts were then compared to the mean values of known secondary structures including a-helix, b-sheet, and random coil. The analysis shows that the peptide's chemical shift is much closer to the values expected in a random coil than in regular secondary structures. Indeed, Ca and C° chemical shifts systematically less than expected a-helical values for more than 1.3 and 0.7 ppm, respectively (Figure 2A). Also, most of the C° chemical shifts for the peptide are 1.0 ppm higher, and Cb shifts are more than 1.0 ppm lower than the expected values for the b-sheet structure (Figure 2B). In turn, comparison with the chemical shifts for the random coil conformation shows small deviations within less than 1 ppm for most of the values (Figure 2C). To summarize the analysis, we calculated the root-mean-square deviations (rmsd) of the experimental chemical shifts from the values expected in different conformations (Figure 2D). The lower rmsd values correspond to the better fit of the peptide's chemical shifts to the chemical shifts expected in a particular conformation of the backbone or a random coil structure (Figure 2D). Thus, the analysis of NMR data suggests that the peptide is very flexible and does not possess extended structured regions. Consistently, in silico protein structure prediction (Iterative Threading ASSEmbly Refinement [I-TASSER]) [11, 12] rendered structures composed primarily of random coils (in white) interrupted by strands (in blue; Figure 2E).

NRVMs exposed to 24 h of hypoxia and incubated with Slt showed improved viability compared to vehicle or a scrambled sequence control (Scr; Figure 3A), particularly when exposed to a concentration of 0.1 μg/mL. Transcriptomic analysis of myocytes exposed to Slt showed a unique gene expression signature compared to vehicle or Scr (Figure 3B). Slt-exposed myocytes upregulated 56 genes and downregulated 110 genes compared to Scr (Figure 3C). Gene Ontology analysis identified biological processes relating to tissue development, cell death and survival, immune development, and function (Figure 3D). Pathway analysis further predicted suppression of stress-induced MAPK-ERK signaling (Figure 3E). This rationalized testing the therapeutic bioactivity of Slt in a rat model of myocardial infarction (MI; Figure 3F). The dose used for MI studies was based on previous investigations of humanin [13], a mitochondrial micropeptide of the same size, where intravenous infusion of 2 mg/kg demonstrated cardioprotective effects [14]. Animals infused with Slt 20 min after reperfusion had decreased infarct size 48 h post-injury compared to vehicle- or Scrinfused animals (Figure 3G, H). Taken together, Slt is cardioprotective both in vitro and in vivo.

2 | MATERIALS AND METHODS

2.1 | Cell culture

Endomyocardial biopsies from the right ventricular aspect of the septum were obtained from two healthy hearts of deceased tissue donors. CDCs were derived as described previously [15]. Briefly, cardiac biopsies were minced into small explants and digested with collagenase. Explants were then cultured on 20 μg/mL fibronectin (BD Biosciences)-coated dishes. Stromal-like flat cells and phase-bright round cells grew out spontaneously from the tissue fragments and reached confluence by 2–3 weeks. These cells were then harvested using 0.25% trypsin (GIBCO) and cultured in suspension on 20 μg/mL poly d-lysine (BD Biosciences) to form self-aggregating cardiospheres. CDCs were obtained by seeding cardiospheres onto fibronectin-coated dishes. All cultures were maintained at 5% CO_2 at 37°C, using Iscove's Modified Dulbecco's Medium (IMDM; Thermo Fisher) supplemented with 20% FBS (HyClone), 1% gentamicin, and 0.1 mL 2-mercaptoethanol.

2.2 | Human CDC and dermal fibroblast micropeptide enrichment

CDCs (passage 4) or normal adult fibrobasts (ATCC; passage 5) were grown to confluence. Cells were then washed several times with IMDM (Thermo Fisher) and then conditioned in IMDM for 15 days. Conditioned media was then harvested and cleared using a 0.45 μm vacuum filter and then stored at −80°C for future use. EV and soluble proteins were precipitated from conditioned media using PEG (1:5 v/v). The pellet was then lysed using Proteomax Surfactant (Promega) at 50°C, for 1 h. A total of 200–250 μg of protein lysate from each sample was then loaded into an Amicon Ultra centrifugal filter (10 kDa; Millipore) and centrifuged per manufacturer's instructions. Flow through (peptide-enriched sample) was then collected for downstream analysis.

2.3 | Mass spectrometry

Peptide-enriched samples were solubilized with 50 mM ammonium bicarbonate, reduced by 1 mM TCEP, alkylated with 4 mM iodoacetamide, and digested with ~1:40 trypsin-LyC (Promega), desalted, and speed vac to total dryness. Liquid chromatography (LC) MS/MS was carried out on a Dionex UltiMate 3000 NanoLC connected to an Orbitrap Elite (Thermo Fisher) equipped with an Easy-Spray ion source. Mobile phase A was comprised of 0.1% aqueous formic acid and mobile phase B was 0.1% formic acid in acetonitrile. Peptides were loaded onto the analytical column (PepMap RSLC C18 2 μm, 100 Å, 50 μm i.d. × 15 cm) at a flow rate of 300 nL/min using a linear AB gradient composed of 2%–25% A for 185 min, 25%–90% B for 5 min, then and isocratic hold at 90% for 5 min with re-equilibrating at 2% A for 10 min. The temperature was set to 40°C for both columns. The nano-source capillary temperature was set to 275°C and the spray voltage was set to 2 kV. MS1 scans were acquired in the Orbitrap Elite at a resolution of 60,000 FWHM with an automated gain control (AGC) target of 1×10^6 ions over a maximum of 500 ms. MS2 spectra were acquired for the top 15 ions from each MS1 scan in normal scan mode in the ion trap with a target setting of 1×10^4 ions, an accumulation time of 100 ms, and an isolation width of 2 Da. The normalized collision energy was set to 35% and one microscan was acquired for each spectra [16]. Preparative data analysis and peptide identification search were performed using the raw MS/MS files after they were converted to mzXML using

MSConvert. The mzXML files were searched against the FASTA from Human Genome Reference consortium release 14 (comprising of 840,6627 proteins and decoys) using the Sorcerer 2-SEQUEST algorithm (Sage-N Research). Target-decoy modeling of peptide spectral matches was performed using the following criteria: fragment tolerance: 1.00 Da; parent tolerance: 0.040–0.160 Da; fixed modification: +57 on C (carbamidomethyl); variable modification: +16 on M (oxidation); enzyme: trypsin with 3 max missed cleavages. Post-search analysis was performed using Scaffold 3 version 1.4.1 (Proteome Software, Inc., Portland, OR, USA) with protein and peptide probability thresholds set to 95%. The MS proteomic data has been deposited to the MassIVE-KB [17] with the dataset identifier MSV000094106.

2.4 | Targeted mass spectrometry in animal tissue

Sample preparation: Tissue was lysed using bead mill tubes resuspended in a 1.1 mL solution of RIPA buffer (Thermo Scientific) and 1x Halt Protease Inhibitor Cocktail (Thermo Scientific). The soluble lysate was then transferred into a 100 kDa Amicon Centrifugal filter unit (Sigma–Aldrich) to filter out large proteins. Flow through was then transferred to a 10 or 3 kDa column for further removal of large proteins. The flow through was then collected for protein digestion and downstream LC-MS/MS.

In solution digestion: Peptides were cleaned by Thermo detergent removal spin columns, then reduced by 5 mM TCEP at 56°C for 1 h and alkylated by 40 mM iodoacetamide at room temperature for 30 min in the dark. Trypsin dissolved in 50 mM of ammonium bicarbonate was added to protein pellets for digestion at 37°C overnight. Digests were desalted by Empore StageTips the following day. Elution from the stage tip was dried by speed vac and re-suspended in 3% acetonitrile with 0.1% formic acid.

LC-MS/MS: 1.0 μg protein was injected into an ultimate 3000 NanoLC, which was equipped with a 75 μm × 2 cm trap column packed with C18 3 μm bulk resins (Acclaim PepMap 100, Thermo Scientific) and a 75 μm × 15 cm analytical column with C18 2 μm resins (Acclaim PepMap RSLC, Thermo Scientific). The NanoLC gradient was 3%–35% solvent B (A = H_2O with 0.1% formic acid; B = acetonitrile with 0.1% formic acid) over 40 min and from 35% to 85% solvent B in 5 min at a flow rate of 300 nL/min. The NanoLC was coupled with a Q Exactive Plus Orbitrap Mass Spectrometer (Thermo Fisher Scientific, San Jose, CA), operated with data dependent acquisition (DDA) mode with an inclusion list for the target peptides. The ESI voltage was set at 1.9 kV, and the capillary temperature was set at 275°C. Full spectra (m/z 350–2000) were acquired in profile mode with resolution 70,000 at m/z 200 with an AGC target of 3×10^6. The most abundant 15 ions were subjected to fragmentation by higher-energy collisional dissociation (HCD) with normalized collisional energy of 25. MS/MS spectra were acquired in centroid mode with a resolution of 17,500 at m/z 200. The AGC target for fragment ions is set at 2×10^4 with a maximum injection time of 50 ms. Charge states 1, 7, 8, and unassigned were excluded from tandem MS experiments. Dynamic exclusion was set at 45.0 s.

Data Analysis: Raw data was searched again for the peptide sequences by Proteome Discovered version 2.5. The following parameters were set: precursor mass tolerance ± 10

ppm, fragment mass tolerance ± 0.02 Th for HCD, up to two miscleavages by semitrypsin, methionine oxidation as variable modification, and cysteine carbamidomethylation as static modification.

2.5 | In silico structure prediction

In silico structure prediction of the structure for Slt was done using the I-TASSER which uses a hierarchical approach to protein structure prediction [11, 12]. This online software platform is generously made available by Dr. Yang Zhang and his group at the Department of Computational Medicine and Bioinformatics at the University of Michigan Medical School: https://zhanggroup.org/I-TASSER/.

2.6 | Peptide synthesis

Slt and Scr peptides used in this paper were prepared using peptide synthesis at the Cedars-Sinai Biomedical Imaging Research Institute. The selected peptides were synthesized by the solid-phase method via the Fmoc strategy, using 2-(1H-benzotriazole-1-yl)–1,1,3,3,-tetramethyluronium hexafluorophosphate (HBTU) as the coupling agent, on a CS136XT automated peptide synthesizer. After appropriate peptide sequences were assembled on Wang Resin, the products were cleaved from the solid support using a TFA cocktail containing 88% trifluoroacetic acid, 5% phenol, 5% water, and 2% tri-isopropylsilane. The crude products were purified by RP-HPLC, using an Apollo C18 column (5 μm, 250 × 10 mm) on an Agilent system. The purified peptides (≥98% HPLC purity) were confirmed by MS measurement of the molecular weights.

2.7 | Nuclear magnetic resonance spectroscopy

The purified peptide was dissolved in 10% D_2O. NMR data have been collected using a 400 MHz Ascent NMR Spectrometer (Bruker) equipped with Prodigy CryoProbe. Topspin, the standard Bruker software, was used for NMR data collection and processing. The following 2D NMR spectra were collected: $^{1}H/^{1}H$-TOCSY (mixing time 80 ms), $^{1}H/^{1}H$-NOESY (mixing time 200 ms), $^{1}H/^{13}C$-HSQC, and $^{1}H/^{13}C$-HMBC. All 2D spectra were collected at 10 and 25°C. The NMR spectra analysis and signal assignment have been performed using the program CARA (The Computer Aided Resonance Assignment Tutorial, R. Keller, Cantina-Verlag, 2004, Switzerland).

2.8 | qPCR

Tissues were homogenized in QIAzol Lysis reagent (Qiagen) using Bead Ruptor 12 (OMNI International) with RNase-free steel beads. RNA was isolated using the miRNeasy Mini kit (Qiagen). RNA was resuspended in 15 μL RNase free water and RNA concentration and purity were determined using a NanoDrop Spectrophotometer (Thermo Scientific). miScript II RT Kit (Qiagen) was used for reverse transcription using 2 μg of isolated RNA for organs 5 × miScript HiFlex Buffer. cDNA was diluted 1:10 for organs for qPCR. qPCR was done with QuantiTect SYBR Green (Qiagen) on QuantStudio 12K Flex or QuantStudio 6 Flex system (Applied Biosystems) with the QuantiMir universal reverse primer, target forward primer (10 μM), and mouse U6 forward primer for the housekeeping gene. qPCR

was run using the following protocol: initial activation step 15 min 95°C, 3-step cycling (denaturation 15 s 94°C, annealing 30 s 60°C, extension 30 s 70°C) for 45 cycles.

2.9 | Neonatal rat ventricular myocyte isolation and micropeptide exposure

NRVMs were isolated as previously described [18]. Briefly, ventricular tissue was harvested from 10 to 20 two-day-old Sprague Dawley rats. Harvested tissue was pooled, minced, and enzymatically digested overnight with Trypsin. Tissue was then sequentially digested with collagenase then quenched with M199 media (10% FBS, glucose, penicillin, vitamin B12, HEPES, and MEM non-essential amino acids; Gibco) and pre-plated to allow attachment of fibroblasts and other non-cardiomyocyte cells. The resulting suspension was collected, counted, and plated for experimental use. NRVMs were cultured at 60%–80% confluence. On the second day post-culture, NRVMs were cultured in reduced serum media (2% FBS) and exposed to vehicle, or 1 μg/mL of Slt or Scr control. Twelve hours later, cells were collected, and washed with phosphate-buffered saline, and RNA was isolated using miRNeasy Mini kit (Qiagen). RNA concentration was ascertained and submitted for RNA sequencing.

2.10 | Next generation sequencing

Total RNA samples were assessed for concentration using a Qubit fluorometer (Thermo Fisher Scientific, Waltham, MA) and for quality using the 2100 Bioanalyzer (Agilent Technologies, Santa Clara, CA). Library construction was performed using the QIAseq Stranded RNA Library kit (Qiagen, Hilden, Germany) with QIAseq FastSelect-rRNA HMR Kit (Qiagen) for ribosomal RNA depletion. Library concentration was measured with a Qubit fluorometer and library size on a Bioanalyzer. Libraries were multiplexed and sequenced on a NovaSeq 6000 (Illumina, San Diego, CA) using 75 bp single-end sequencing. On average, approximately 50 million reads were generated from each sample. Raw sequencing data were demultiplexed and converted to FASTQ format by using bcl2fastq v2.20 (Illumina, San Diego, California). Then reads were aligned to the GRCm38 reference genome (http://www.gencodegenes.org) using STAR (version 2.6.1)4 with default parameters. Gene expression was quantified by RSEM (version 1.2.28)5 to generate a raw count expression matrix with gene identities as rows and samples as columns. DESeq2 (version 1.26.0)6 was used to normalize the raw count expression and correct the batch effect.

2.11 | Gene Ontology analysis

Gene Ontology analysis was performed using Ingenuity Pathway Analysis software (Qiagen). Evaluated genes included all genes up and downregulated by a fold change of at least two and a *p*-value difference of 0.05 or less (95% CI).

2.12 | Primary rat ventricular cardiomyocyte culture and hypoxia model

Neonatal rat ventricular cardiomyocytes (NRVMs) were isolated as described above. After 24 h left undisturbed in a 5% CO_2 incubator, unattached cells and debris were removed by aspiration, and fresh media was added. Two days later, media was replaced with a 1% FBS media overnight. Then, treatment with Scr or Slt (1, 10, 50, and 100 ng/mL) was

initiated 4 h before hypoxia induction (94% N_2, 5% CO_2, and 1% O_2) for 24 or 48 h. Some plates were allowed to recover in normoxia condition (reoxygenation). For the control group (normoxia), the cells were kept in a standard incubation chamber (5% CO_2, and 21% O_2) for an identical period. Cell viability was determined by cell counting kit 8 (CCK8; Sigma–Aldrich) following the manufacturer's recommendation. Each condition tested was performed in five replicates.

2.13 | Animal studies

All animal studies were conducted under approved protocols from the Institutional Animal Care and Use Committee at Cedars-Sinai Medical Center.

2.14 | Rat ischemic-reperfusion model with retro-orbital injection

To induce ischemia/reperfusion (I/R) injury, 7–10-week-old female Wistar Kyoto rats were provided general anesthesia, and then a thoracotomy was performed at the 4th intercostal space to expose the heart and left anterior descending coronary artery. A 7–0 silk suture was then used to ligate the left anterior descending coronary artery, which was subsequently removed after 45 min to allow for reperfusion for 20 min. The animal surgeon was blinded to treatment groups. At 20 min, animals were given vehicle (saline) or 300 μg of Slt or a Slt sequence Scr control (Scr) without the use of a transfection reagent. After 48 h the animals were sacrificed. Blood was collected immediately before euthanasia for serum testing and the heart was removed intact post-mortem for TTC staining.

2.15 | ELISA

Cardiac Troponin ELISA (R&D Systems, Quantikine ELISA) was performed according to the manufacturer's protocol. The sample concentration for testing was 1.2 mg/mL.

2.16 | TTC staining

Two days following the I/R injury, animals were euthanized by cervical dislocation. Then, hearts were harvested, washed in PBS, and cut into 1-mm sections from apex to base, above the infarct zone. Sections were incubated with 1% solution 2,3,5-triphenyl-2H-tetrazolium chloride (TTC) for 30 min at 37°C in the dark, washed with PBS, and then fixed overnight at 4°C in 4% paraformaldehyde. Then, sections were imaged and weighed. The infarcted zones (white) were delineated from viable tissue (red) and analyzed (ImageJ software). Infarct mass was calculated in the tissue sections according to the following formula: (infarct area/tot area)/section weight (mg).

2.17 | Statistics

GraphPad Prism 9.0 (GraphPad Software) was used to analyze the data. Comparison of three or more groups was performed using two- or one-way analysis of variance (ANOVA) Tukey's post hoc multiple comparison tests for paired groups. Comparisons of two groups were done using an unpaired two-tailed Student's *t*-test with a 95% confidence interval.

3 | RESULTS/DISCUSSION

In conclusion, here we describe a novel long non-coding RNA-derived micropeptide, Slt, within the CDC secretome. Structural analysis reveals that Slt is flexible, as is true for most micropeptides [19]. However, it is important to note the NMR analysis was done on a synthetically prepared peptide, which may exclude post-translational modifications that may otherwise endow Slt with a more rigid secondary structure. Future investigations will involve structural resolution of Slt using a recombinant protein, derived from a eukaryotic expression host system such as yeast. The cytoprotective effects exerted by Slt in vitro and transcriptomic data suggest a potent tissue protective capacity. However, future studies are needed to evaluate protein binding targets of Slt in cardiomyocytes and how such interactions may impact cardiomyocyte inflammation. More broadly, further investigation will be needed to identify critical target cells and tissue in Slt-mediated cardioprotection in vivo.

Supplementary Material

Refer to Web version on PubMed Central for supplementary material.

ACKNOWLEDGMENTS

The authors thank the Cedars-Sinai Proteomics and Metabolomics Core for access to the various mass spectrometers, Cedars-Sinai Genomics Core for support with RNA sequencing, Yi Zhang of the Cedars-Sinai Biomedical Imaging Research Institute for peptide synthesis, and Weixin Liu for technical assistance. The authors also thank Rodrigo Miguel dos Santos for help with the NRVM hypoxia assay. Schematic figures were created using BioRender.com. Financial support for this work was provided by National Institutes of Health Grants R01HL142579, R01 T32 HL116273, 1 R01 HL155346-01, and the California Institute for Regenerative Medicine EDUC4-12751.

Funding information

National Institutes of Health, Grant/Award Numbers: R01HL142579, R01 T32 HL116273, 1 R01 HL155346-01; California Institute for Regenerative Medicine, Grant/Award Number: EDUC4-12751; National Heart, Lung, and Blood Institute, Grant/Award Numbers: R01 HL142579, R01 HL155346-01, R01 T32 HL116273

DATA AVAILABILITY STATEMENT

All data are provided in the main figures and supporting information. The MS proteomics has been deposited to MassIVE-KB (ID MSV000094106).

Abbrevations:

AGC	automated gain control
BLAST	Basic Local Alignment Search Tool
CDC	cardiosphere-derived cells
DDA	data dependent acquisition
EV	extracellular vesicle

HBTU	2-(1H-benzotriazole-1-yl)–1,1,3,3,-tetramethyluronium hexafluorophosphate
HCD	higher-energy collisional dissociation
I/R	ischemia/reperfusion
IMDM	Iscove's Modified Dulbecco's Medium
I-TASSER	Iterative Threading ASSEmbly Refinement
LINC	long intergenic non-coding
MI	myocardial infarction
NRVM	neonatal rat ventricular myocyte
rmsd	root-mean-square deviations
Scr	scramble
Slt	slitharin
sORF	small open reading frame
UTR	untranslated region

REFERENCES

1. Makarewich CA, & Olson EN (2017). Mining for micropeptides. Trends in Cell Biology, 27(9), 685–696. 10.1016/j.tcb.2017.04.006 [PubMed: 28528987]
2. Saghatelian A, & Couso JP (2015). Discovery and characterization of smORF-encoded bioactive polypeptides. Nature Chemical Biology, 11(12), 909–916. 10.1038/nchembio.1964 [PubMed: 26575237]
3. Andrews SJ, & Rothnagel JA (2014). Emerging evidence for functional peptides encoded by short open reading frames. Nature Reviews Genetics, 15(3), 193–204. 10.1038/nrg3520
4. Anderson DM, Anderson KM, Chang C-L, Makarewich CA, Nelson BR, Mcanally JR, Kasaragod P, Shelton JM, Liou J, Bassel-Duby R, & Olson EN (2015). A micropeptide encoded by a putative long noncoding RNA regulates muscle performance. Cell, 160(4), 595–606. 10.1016/j.cell.2015.01.009 [PubMed: 25640239]
5. Bi P, Ramirez-Martinez A, Li H, Cannavino J, Mcanally JR, Shelton JM, Sánchez-Ortiz E, Bassel-Duby R, & Olson EN (2017). Control of muscle formation by the fusogenic micropeptide myomixer. Science, 356(6335), 323–327. 10.1126/science.aam9361 [PubMed: 28386024]
6. Aminzadeh MA, Rogers RG, Fournier M, Tobin RE, Guan X, Childers MK, Andres AM, Taylor DJ, Ibrahim A, Ding X, Torrente A, Goldhaber JM, Lewis M, Gottlieb RA, Victor RA, & Marbán E (2018). Exosome-mediated benefits of cell therapy in mouse and human models of duchenne muscular dystrophy. Stem Cell Reports, 10(3), 942–955. 10.1016/j.stemcr.2018.01.023 [PubMed: 29478899]
7. Ibrahim AG-E, Cheng K, & Marbán E (2014). Exosomes as critical agents of cardiac regeneration triggered by cell therapy. Stem Cell Reports, 2(5), 606–619. 10.1016/j.stemcr.2014.04.006 [PubMed: 24936449]
8. Kearse MG, & Wilusz JE (2017). Non-AUG translation: A new start for protein synthesis in eukaryotes. Genes & Development, 31(17), 1717–1731. doi:10.1101/gad.305250.117 [PubMed: 28982758]

9. Németh AL, Medveczky P, Tóth J, Siklódi E, Schlett K, Patthy A, Palkovits M, Ovádi J, Tõkési N, Németh P, Szilágyi L, & Gráf L (2007). Unconventional translation initiation of human trypsinogen 4 at a CUG codon with an N-terminal leucine. The FEBS Journal, 274(6), 1610–1620. 10.1111/j.1742-4658.2007.05708.x [PubMed: 17480209]
10. Starck SR, Jiang V, Pavon-Eternod M, Prasad S, Mccarthy B, Pan T, & Shastri N (2012). Leucine-tRNA initiates at CUG start codons for protein synthesis and presentation by MHC class I. Science, 336(6089), 1719–1723. 10.1126/science.1220270 [PubMed: 22745432]
11. Yang J, Yan R, Roy A, Xu D, Poisson J, & Zhang Y (2015). The I-TASSER Suite: Protein structure and function prediction. Nature Methods, 12(1), 7–8. 10.1038/nmeth.3213
12. Zhou X, Zheng W, Li Y, Pearce R, Zhang C, Bell EW, Zhang G, & Zhang Y (2022). I-TASSER-MTD: A deep-learning-based platform for multi-domain protein structure and function prediction. Nature Protocols, 17(10), 2326–2353. 10.1038/s41596-022-00728-0 [PubMed: 35931779]
13. Ying G, Iribarren P, Zhou Y, Gong W, Zhang N, Yu Z-X, Le Y, Cui Y, & Wang JM (2004). Humanin, a newly identified neuroprotective factor, uses the G protein-coupled formylpeptide receptor-like-1 as a functional receptor. Journal of Immunology, 172(11), 7078–7085. 10.4049/jimmunol.172.11.7078
14. Muzumdar RH, Huffman DM, Calvert JW, Jha S, Weinberg Y, Cui L, Nemkal A, Atzmon G, Klein L, Gundewar S, Ji SY, Lavu M, Predmore BL, & Lefer DJ (2010). Acute humanin therapy attenuates myocardial ischemia and reperfusion injury in mice. Arteriosclerosis, Thrombosis, and Vascular Biology, 30(10), 1940–1948. 10.1161/ATVBAHA.110.205997 [PubMed: 20651283]
15. Makkar RR, Smith RR, Cheng K, Malliaras K, Thomson LE, Berman D, Czer LS, Marbán L, Mendizabal A, Johnston PV, Russell SD, Schuleri KH, Lardo AC, Gerstenblith G, & Marbán E (2012). Intracoronary cardiosphere-derived cells for heart regeneration after myocardial infarction (CADUCEUS): A prospective, randomised phase 1 trial. Lancet, 379(9819), 895–904. 10.1016/S0140-6736(12)60195-0 [PubMed: 22336189]
16. Wang M, Wang J, Carver J, Pullman BS, Cha SW, & Bandeira N (2010). Assembling the community-scale discoverable human proteome. Journal of Biological Chemistry, 285(6), 412–421.e5. doi:10.1074/jbc.M109.068577
17. Wang M, Wang J, Carver J, Pullman BS, Cha SW, & Bandeira N (2018). Assembling the community-scale discoverable human proteome. Cell Systems, 7(4), 412–421.e415. 10.1016/j.cels.2018.08.004 [PubMed: 30172843]
18. Sekar RB, Kizana E, Cho HC, Molitoris JM, Hesketh GG, Eaton BP, Marbán E, & Tung L (2009). IK1 heterogeneity affects genesis and stability of spiral waves in cardiac myocyte monolayers. Circulation Research, 104(3), 355–364. 10.1161/CIRCRESAHA.108.178335 [PubMed: 19122180]
19. Tharakan R, & Sawa A (2021). Minireview: Novel micropeptide discovery by proteomics and deep sequencing methods. Frontiers in Genetics, 12, 10.3389/fgene.2021.651485

STATEMENT OF CLINICAL RELEVANCE

Cardiosphere-derived cells (CDCs) are a population of cardiac stromal cells with pre-clinical and clinical-demonstrated tissue reparative capacity. CDCs exert their effects through the secretion of paracrine factors which include extracellular vesicles and soluble protein factors. In this study, we probed the secretome of CDCs to identify potential micropeptides which might contribute to the therapeutic bioactivity of CDCs. We identified a 24-residue micropeptide (dubbed slitharin [Slt]) which derives from the long non-coding RNA gene LINC02099. Its demonstrated therapeutic activity in a rat model of myocardial infarction points to a putative role in CDC-mediated cardiac tissue repair. Though the mechanism of Slt signaling remains to be elucidated, this discovery sheds new light on the role of micropeptides in the indirect effect of therapeutic cells and offers a novel discovery paradigm for micropeptides with therapeutic bioactivity.

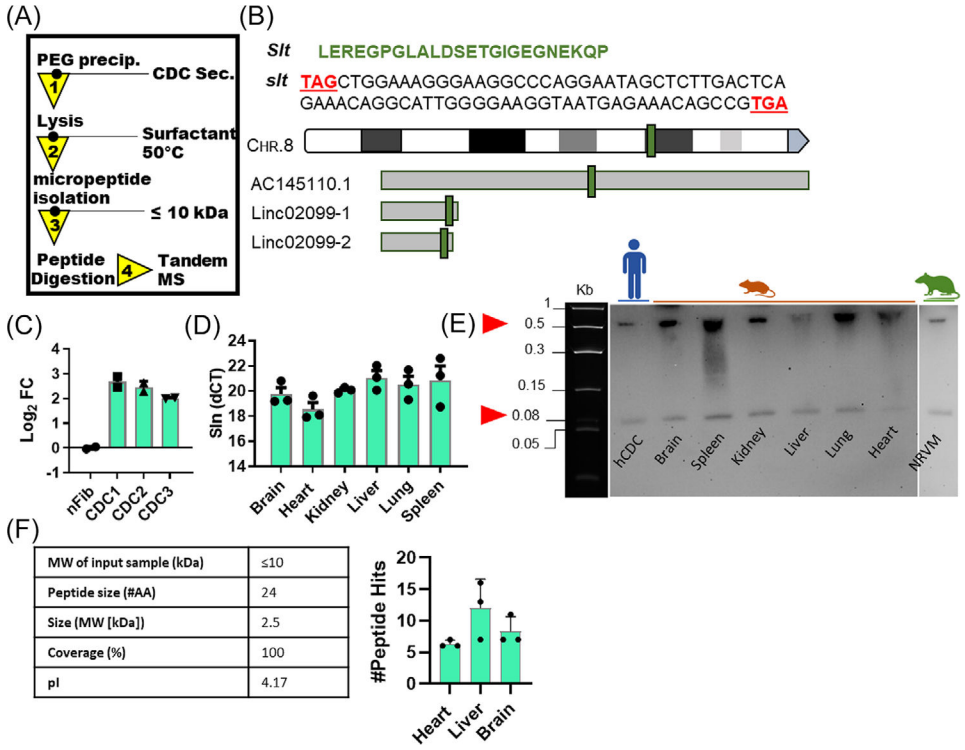

FIGURE 1.

Slitharin (Slt) is a secreted micropeptide originating from a small open reading frame in long intergenic non-coding (LINC) RNA 02099. (A) Schematic of the micropeptide screening preparation from the conditioned media of cardiosphere-derived cells (CDC); (B) peptide sequence of Slt (above), the mRNA sequence (middle; stop codons are denoted in red font), and the location of this sequence in the human genome (p-arm of chromosome 8, and three sites where the sequence occurs (green bars denote location along the length of the gene). (C) gene expression of Slt in normal human fibroblasts compared to three human CDC donor lines ($n = 3$ replicates per group). (D) Gene expression of Slt in mouse tissue (U6 as a reference; $n = 3$ biological replicates per group). (E) Northern blot showing the presence of 0.5 kb and 80 bp nucleotide transcript of the Slt sequences in human CDCs, mouse tissue, and rat neonatal ventricular myocytes (SYBR Green stained gel ladder used for size reference). (F) Targeted mass spectrometry of Slt demonstrating detection of target peptide in mouse tissue (table on the left represents parameters for peptide detection; each data point represents tissue from one animal).

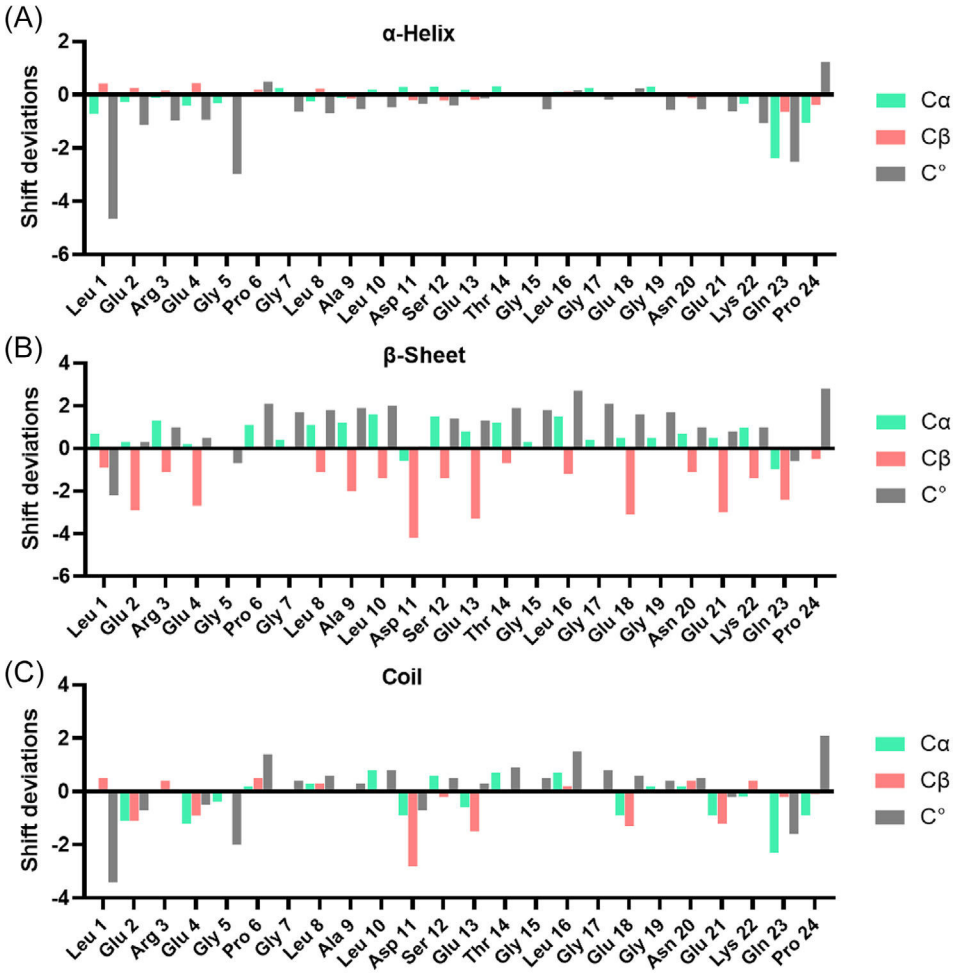

(D)

Atoms	Secondary structure			mean*
	α-helix	β-sheet	coil	
Cα	2.58	0.89	0.76	0.60
Cβ	0.94	2.11	0.92	0.26
C^{O}	2.10	1.62	1.15	1.38
Total	2.05	1.58	0.96	0.91

(E)

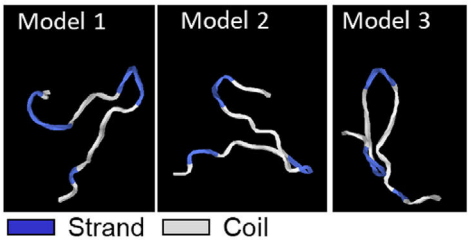

FIGURE 2.

Slitharin (Slt) adopts a flexible coiled structure. Deviations of the chemical shifts of the peptide from the chemical shifts expected for α-helix (A), β-sheet (B), and random coil (C). Blue, orange, and gray bars represent the data for Ca, Cb, and C° atoms, respectively. (D) Root-mean-square deviations (rmsd) for the chemical shift of the peptide HN-24 from the mean statistical values (*the mean value for all peptide/protein chemical shifts in the database). (E) Top three in silico structure predictions of the structure of Slt (random coil in white and strands in blue).

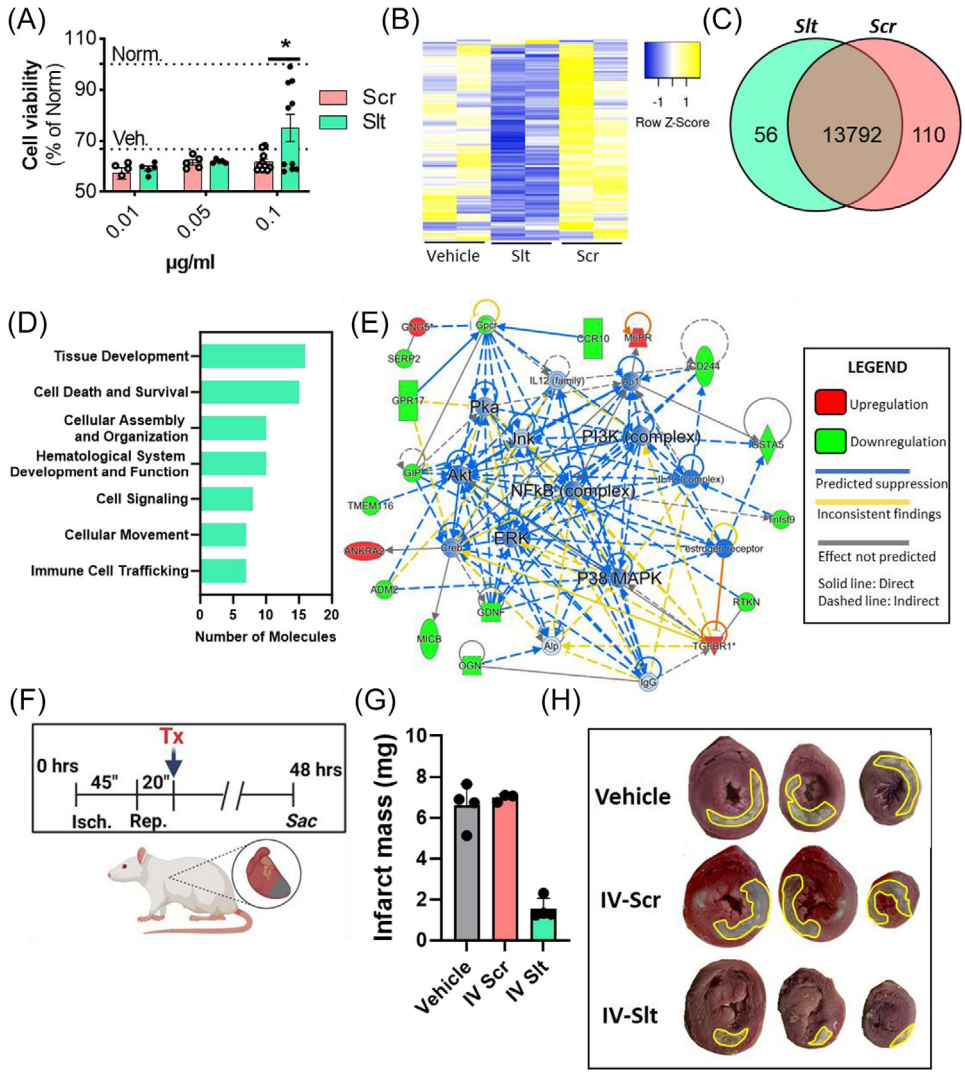

FIGURE 3.

Slitharin (Slt) suppresses stress-induced MAPK-ERK signaling and exerts cardioprotective effects in a rat model of myocardial infarction. (A) Slt improves viability in hypoxic neonatal rat ventricular myocytes (NRVMs) (n = 5–10 replicates per group). (B) Heatmap showing differential gene expression in NRVMs treated with vehicle, Slt, or an Slt-scrambled sequence (scramble [Scr]). (C) Venn diagram showing differentially expressed genes between Slt- and Scr-treated NRVMs. Gene Ontology analysis identifying the top enriched biological processes in Slt-treated NRVMs compared to Scr. (D) Top predicted pathway affected by Slt treatment in NRVMs. (E) Pathway network showing suppression of MAP-ERK and NFkB signaling in Slt-exposed NRVMs compared to scramble. (F) Schematic for the rat myocardial infarction study. Animals received ischemic injury for 45 min followed by reperfusion. Animals received Slt, Scr, or vehicle 20 min post-reperfusion and sacrificed 48 h post-injury (n = 3–4 animals per group). (G, H) Bars represent mean values and error bars represent standard errors of the mean. Comparisons were done using a

one-way analysis of variance (ANOVA) with Tukey's post-test; *$p < 0.05$, **$p < 0.01$, ***$p < 0.001$.